SIAM J. SCI. COMPUT.
Vol. 21, No. 3, pp. 799–818

AN ADAPTIVE FINITE ELEMENT METHOD FOR UNSTEADY CONVECTION-DOMINATED FLOWS WITH STIFF SOURCE TERMS*

FRIEDRICH K. HEBEKER† AND ROLF RANNACHER‡

Abstract. We consider nonstationary convection-dominated flows with stiff source terms. As a unified approach to such problems a combined finite element method in space and time with streamline diffusion is examined numerically. It has good shock-capturing features and is implicit and L-stable. Moreover, being a Galerkin method, it admits residual-based weighted a posteriori error estimates of optimal order. We avoid the use of *global* stability constants by actually solving the dual problem. This in turn leads to efficient and mathematically rigorous mesh refinement strategies where the streamline diffusion parameter is used for optimizing the resulting adaptive scheme. All theoretical results are substantiated by numerical test examples. For a physical application, we turn to detonation waves at moderate relaxation times in one space dimension. The finite element method well reproduces the Chapman Jouguet speed of detonations and their wave structure. Our error estimator proves accurate and sensitive to parameters, at least on time intervals of moderate length. The adaptive scheme based on this estimator produces fairly accurate results which appear to be the best available with the present strategy. All ingredients of the numerical scheme can be extended in a natural way to higher space dimensions.

Key words. adaptive finite elements, a posteriori error analysis, duality arguments, convection-dominated flows, detonation waves, discontinuous Galerkin method, streamline diffusion

AMS subject classifications. 65M60, 76M10, 80A32

PII. S1064827597319039

1. Introduction.

We consider a system of convection-diffusion-reaction equations

$$u_t + f(u)_x = Du_{xx} - \frac{1}{\tau}g(u) \quad \text{in} \quad \Omega \times I, \tag{1.1}$$

where $u = u(x,t)$ is a d-dimensional vector function, while $f, g : \mathbb{R}^d \to \mathbb{R}^d$ are nonlinear vector mappings (f assumed as smooth, say, of class C^∞). As long as the meaning is clear, the notation used below does not distinguish between scalar and vector functions. This system is given on a bounded open domain $\Omega \times I = (0,1) \times (0,T)$ in the (x,t)-plane. The parameters, assumed to be constant, are the *diffusion coefficients* and the *relaxation time*

$$D = \operatorname{diag}(\epsilon_1, \dots, \epsilon_d), \qquad 0 < \epsilon_i \ll 1, \qquad 0 < \tau \ll 1.$$

Equation (1.1) is supplemented by initial and boundary conditions

$$u|_{t=0} = u_0, \qquad u|_{\partial\Omega} = 0, \tag{1.2}$$

*Received by the editors March 20, 1997; accepted for publication (in revised form) October 13, 1998; published electronically November 4, 1999. This work was supported by the Deutsche Forschungsgemeinschaft (DFG), SFB 359, "Reaktive Strömungen, Diffusion und Transport," Universität Heidelberg.

http://www.siam.org/journals/sisc/21-3/31903.html

†Fachbereich Mathematik, Universität Giessen, Arndtstr. 2, D-35392 Giessen, Germany (friedrich.k.hebeker@math.uni-giessen.de).

‡Institut für Angewandte Mathematik, Universität Heidelberg, INF 294, D-69120 Heidelberg, Germany (rannacher@iwr.uni-heidelberg.de).

which are appropriately modified in the limiting case $\epsilon_i = 0$, $i = 1, ..., d$.

System (1.1) is singularly perturbed in two ways and poses several unique and rarely tackled difficulties to rigorous numerical analysis, even in the spatially one-dimensional case considered here. In past decades, successful numerical approaches have been developed to address (nonlinear) fluxes $f(u)$ [17, 19]. In the present study, we concentrate rather on certain effects due to the stiff source term $\frac{1}{\tau}g(u)$. Examples include "geometrical sources," e.g., radially symmetric flows or those with dimension reduction (quasi-one-dimensional flows) or, more complex, currents in semiconductors (see the overview article [25]) or chemically reacting flows, e.g., detonation problems, [5, 7] and [13]. An example for the latter will be considered below in more detail. For a typical industrial application, we refer to [15]. In this paper, we will develop a new approach to solving problems of this type by a finite element Galerkin method with emphasis on adaptive mesh-size selection and rigorous a posteriori error control. For expository reasons, we confine ourselves to the spatially one-dimensional case. However, the essential features of our approach can be generalized in a natural way to higher dimensions.

From the point of view of mathematical analysis, system (1.1) seems to be well understood in the spatially one-dimensional case if the data are sufficiently smooth and ϵ_i, $\tau > 0$. For instance, (1.1) with (1.2) has a unique generalized solution globally in time, if $u_0 \in H^1(\Omega)$ [1]. Algebraic stability conditions have been introduced in [32] to investigate analytically the limiting behavior in case of $\tau \to 0$. Unfortunately, in many applications, systems like (1.1) do not satisfy such criteria in physically interesting cases (e.g., in a detonation model where the internal energy exceeds the equilibrium value). The basic numerical difficulties posed by (1.1) are as follows:

- Boundary layers, shocks, and even *spikes* may appear (for vanishing diffusion).
- The system is highly *nonlinear*, with (nearly) irregular nonlinearity g.
- The system is *stiff*, since $\tau \ll 1$.
- *Unphysical wave speeds* are sometimes observed, thus possibly destroying all information of the numerical result.

The last problem, in particular, is typical of systems like (1.1) in case of specific source terms. This problem is fundamental, not just typical for a given numerical approach and is of great influence even for moderate values of τ. Colella, Majda, and Roytburd [6] were seemingly the first to observe the phenomenon of artificial wave speeds while investigating a simplified model of reacting shock waves. By employing (now standard) finite volume schemes and operator splitting they concluded that for very fine meshes the ZND wave (named after Zel'dovich, von Neumann, and Döring) is completely resolved by these methods, but for moderately fine meshes the numerical wave structure is moving at mesh speed. This effect has been further clarified by LeVeque and Yee [24] by considering a relatively simple example to be recalled here briefly. Let us consider the scalar equation

$$u_t + u_x = -\frac{1}{\tau}u(u - 0.5)(u - 1) \tag{1.3}$$

with appropriate boundary conditions ($\tau > 0$ a small constant parameter) and the initial data prescribed as $u_0(x) = 1$ for $x < 0$, and $u_0(x) = 0$ otherwise. The analytical solution is the traveling wave $u(x, t) = u_0(x - t)$. Numerical solution would introduce some smearing, so the source term becomes active. Since the values of $u = 0$ and $u = 1$ are stable equilibria (whereas $u = 0.5$ is unstable), the shock profile is essentially preserved if τ is chosen sufficiently small. But the accidental distribution of numerical diffusion generates a nonphysical wave propagation. Thus we may think

of some "catastrophic" interaction between numerical diffusion and reaction terms (see the investigation of [24]). Evidently, this defect is neither due to nonlinearity nor to a specific way of numerical approximation. Rather, we are dealing with a genuine feature of instability of the present problem. In practical situations this effect might be overshadowed by different phenomena, but it should be taken into account in any case. In simple cases the artificial wave speed might be estimated if the approximate formulae available for the resulting nonlinear eigenvalue problem for the wave speed are evaluated explicitly [12].

Several recent papers on reactive flows assume a sharp reaction front and thus combine solving conservation laws without source terms with computing the discontinuity by shock tracking (cf. [16] and recent papers cited there). Pember [26] provides an investigation on the limiting behavior for $\tau \to 0$ of a (simpler) relaxation problem by means of finite volume schemes with different kinds of operator splitting.

The consequences we draw from the phenomenon described above for algorithmic development by far exceed mere accuracy requirements. In fact, there seems to be some inherent *physical instability* ((1.1) appears also in certain models of phase transition, cf. [9, 23]), so we are led to design algorithms which actually have to *minimize the required numerical diffusion!*

Our numerical approach to solving (1.1) is the *streamline diffusion finite element method* (*SDFEM*), a finite element method in space and time, introduced by Hughes, Franca, and Mallet [18] and Johnson [19] for convection-dominated flows. It is implemented here for the spatially one-dimensional case, but it should be noted that all techniques developed in this note (at least in principle) can be extended to higher space dimensions. We use a quadrangulation of the domain in the (x, t)-plane (allowing for hanging nodes) and employ piecewise bilinear and possibly discontinuous-in-time trial functions (the so-called $DG(1)$-method). Salient features of this method are its inherent

- insensitivity to long-time computation (even in the presence of diffusion),
- sharp and reliable weighted a posteriori error estimates, and consequently,
- adaptive discretization schemes using residual-based error control.

For the latter, we use the recent approach by [2] based on *weighted a posteriori error estimates* which entails the numerical solution of a (linear) *dual problem.* (Combining the original with some dual problem is a well-known technique, for instance, in optimization theory.) The information carried by the dual solution is explicitly used in the form of local weights in our a posteriori error bounds. This combined analysis allows us to avoid stability constants as they appear in the general approach by Eriksson et al. [10] (see also [30]), since accurate estimates of those are hardly available for nonlinear problems. Moreover, this concept seems to be particularly useful in case of strongly nonhomogeneous behavior of the original problem as in the present case. The dual problem is solved numerically in coarser approximation only, in order to keep the additional effort low. This is a very crucial aspect of the whole approach. It is expected to be justified as the time step is taken relatively small and the dual solution enters only through the weights in the a posteriori error estimates. Thus, the present method should be well adapted (at least conceptionally) to the task of unphysical wave speeds. In this respect, we point to the important role played by the streamline diffusion parameter δ (see section 2 below). Essentially a free parameter, we use it to *optimize the adaptive procedure* by adjusting the required numerical diffusion. Concerning further examples of the method of weighted a posteriori error estimates applied to various physical problems including elastoplasticity, radiative transfer, and

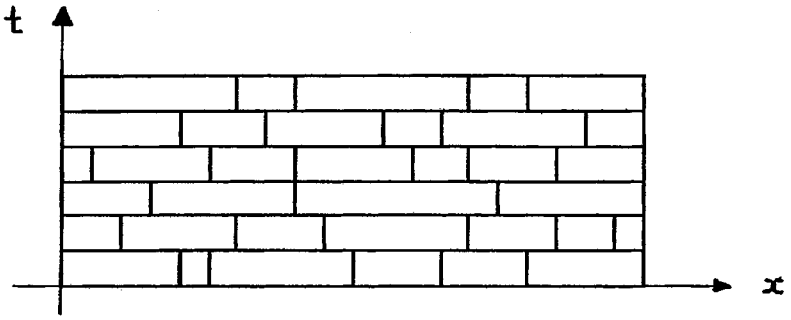

FIG. 1. *Quadrangulation Q in (x,t)-space.*

viscous incompressible flows, we refer to [2, 3, 21, 28]. In [11] a lot of numerical experience with problems of classical gas dynamics is provided.

The present paper is organized as follows: In section 2, we introduce the streamline diffusion finite element method. In section 3, we develop the corresponding a posteriori error analysis which serves as basis of the adaptive algorithm which is introduced and discussed in section 4. In the concluding section 5, we investigate detonation waves as a test example. Several numerical tests confirm the usefulness of our strategy for error control and grid adjustment.

2. SDFEM. Our method for discretization of problem (1.1) is the SDFEM, a finite element method in space and time, using a quadrangulation of the domain in the (t,x)-plane and employing piecewise bilinear trial functions possibly discontinuous in time (the so-called $DG(1)$-method). Let

$$0 = t_0 < t_1 < \cdots < t_N = T$$

be a set of discrete time levels, with corresponding time intervals $I_n = (t_{n-1}, t_n]$ and time steps $k_n = t_n - t_{n-1}$. For practical computation, we confine ourselves to constant (sufficiently small) time-step sizes $k_n \equiv k$. We associate with each time interval I_n a decomposition of Ω into $M_n + 1$ space intervals $I_{n,l} = (x_{n,l-1}, x_{n,l}]$, $l = 1, \ldots, M_{n+1}$, of length $h_{n,l}$. The space-time mesh size is sometimes denoted symbolically as $h = h(x,t)$. Accordingly, the elements of the local quadrangulation Q_n on the nth time slab are rectangles $K_{n,l} = I_{n,l} \times I_n$. All local quadrangulations Q_n combined form the *quadrangulation* Q of $\Omega \times I$ consisting of elements K (see Figure 1).

Let $|\cdot|$ denote the Euclidean vector norm. Given a Lipschitz-bounded open set Q, we will denote by $L^2(Q)$ and $H^1(Q)$ the usual Hilbert spaces of functions (or vector fields) which are square-integrable or along with their first generalized derivatives square-integrable on Q, while $H_0^1(Q)$ contains the functions of $H^1(Q)$ which vanish along the boundary. $\|\cdot\|_{L^2(Q)}$ denotes the $L^2(Q)$-norm of a function (or vector field), which is mostly abbreviated by $\|\cdot\|_Q := \|\cdot\|_{L^2(Q)}$. We will use the notation $(\cdot,\cdot) = (\cdot,\cdot)_\Omega$ for the inner product of $L^2(\Omega)$ and $\|\cdot\| = \|\cdot\|_\Omega$ for the corresponding norm. Further, we define the time-space inner product

$$(\cdot,\cdot)_n := \int_{I_n} (\cdot,\cdot)\, dt.$$

An important role is played by the space

$$V = \{v \in H^1(\Omega \times I) :\ v|_{\partial\Omega} = 0\}.$$

For discretization we use

$$W_n := \{w \in H_0^1(\Omega) : w|_{I_{n,l}} \text{ linear } \ \forall l = 1, \dots, M_{n+1}\},$$

the standard finite element space of continuous, piecewise linear trial functions, vanishing on $\partial\Omega$. On each time slab $I_n \times \Omega$, we now introduce the finite element space

$$V_n := \{v \in H^1(\Omega \times I_n) : \ v(x,t) = w_0(x) + tw_1(x), \ w_i \in W_n\},$$

and we let

$$V_h := \{v : \Omega \times I \to \mathbb{R}^d : \ v|_{\Omega \times I_n} \in V_n, \ 1 \le n \le N\}.$$

Then, the SDFEM reads as follows: Find $U \in V_h$, so that

$$A_\delta(U; v) = L(v) \quad \forall\, v \in V_h. \tag{2.1}$$

Here, for fixed U, $A_\delta(\cdot;\cdot)$ denotes the semilinear form

$$A_\delta(w; v) := \sum_{n=1}^{N} \left\{ \left(w_t + f(w)_x + \frac{1}{\tau} g(w), v + \delta\{v_t + f'(U)^T v_x\} \right)_n + (Dw_x, v_x)_n \right\} + \sum_{n=1}^{N-1} ([w]_n, v_n^+) + (w_0^+, v_0^+)$$

and $L(\cdot)$ the linear functional

$$L(v) := (u_0, v_0^+).$$

By $A_0(\cdot;\cdot)$, we will denote the unperturbed form, with $\delta = 0$. We further use the abbreviations

$$v_n := v(\cdot, t_n), \qquad v_n^+ := \lim_{t \to t_n + 0} v(\cdot, t), \qquad v_n^- := \lim_{t \to t_n - 0} v(\cdot, t), \qquad [v]_n := v_n^+ - v_n^-.$$

We emphasize that, since the test functions v in (2.1) are chosen discontinuous in time, the algebraic system decouples in time. Thus, it results in a familiar implicit time stepping scheme, advancing the discrete solution U from one time level to the next. In fact, as a time discretization, the DG(1) method just corresponds to a variant of the subdiagonal (2, 1)-Padé approximation of the exponential [4, 8]. Therefore, the scheme is quite costly. It is implicit and employs two variables for all physical quantities at all time levels t_n. On the other hand, such Padé approximations lead to L-stable time stepping schemes, a property strongly required for stiff differential equations [31]. More economical extensions of the scheme while retaining its favorable properties (e.g., variants in the sense of Hairer's Radau quadrature and Butcher's SIRK method) are left to future work.

This SDFEM formulation corresponds to a (perturbed) Petrov–Galerkin scheme in space-time, due to presence of the δ-term which stabilizes the unstable standard Galerkin scheme (least-squares stabilization). We refer to δ as the *streamline diffusion parameter*, usually of size $\delta = c_{sd}h$ (cf. [20, 29, 33]), which will play a fundamental role in our numerical procedure.

The *practical implementation* of SDFEM requires a conservative variant to handle the convective term. We replace the term $f(u)_x v$ in (2.1) by $-f(u)v_x$ and the term

(u_t, v) by $-(u, v_t)$. In the nonlinear case (with vanishing g) this results in a *conservative scheme* even in the case of linearized implementations of $f(u)$ [11]. Further, the *shock-capturing* modification of the diffusion part (cf. [20]) has been implemented, where the diffusion parameter D is modified according to

$$\hat{D} := \mathrm{diag}(\hat{\epsilon}_i), \qquad \hat{\epsilon}_i := \max\left\{\epsilon_i,\, c_{def}\frac{hR(U)}{|\nabla U| + h}\right\},$$

where, on each space-time element K

$$R(U) := \left|U_t + f(U)_x + \frac{1}{\tau}g(U)\right| + |k_K^{-1}[U]_n|,$$

and $c_{def} := c_{sd}$. However, this modification will not be explicitly considered in our a posteriori error analysis, below.

The SDFEM forms an algebraic system decoupled in time, hence resulting in nonlinear banded systems to be solved independently for each time step. In the given case of moderate relaxation times τ the linear iteration suffices to solve the system in few (generally about two) iteration steps.

Our numerical test example with detonation waves (see Figure 2) on a uniform and fine mesh (at moderate relaxation time $\tau = 10^{-1}$) illustrates that the SDFEM is quite appropriate for dealing with such intricate physical phenomena like propagating detonation waves. In the following sections we are searching for methods to improve the SDFEM from an economical point of view.

3. A posteriori error analysis. Accurate residual-based error control is based on a combined study of the original problem with some "dual" problem (for reasons explained in the introduction) and the use of *Galerkin orthogonality* inherent to the SDFEM. To find the appropriate dual problem, we proceed as follows. Given u and U, the form $B(u, U; w, v)$ which is linear in the last two arguments has to satisfy the equation

$$A_0(u; v) - A_0(U; v) = B(u, U; e, v), \qquad v \in V, \tag{3.1}$$

for $w = e := u - U$. Elementary analysis shows that

$$B(u, U; w, v) = \sum_{n=1}^{N}\left\{(w_t, v)_n - (Mw, v_x)_n + \frac{1}{\tau}(Nw, v)_n + (Dw_x, v_x)_n\right\} + \sum_{n=1}^{N-1}([w]_n, v_n^+) + (w_0^+, v_0^+),$$

with the matrices

$$M := \int_0^1 f'(su + (1-s)U)\, ds, \qquad N := \int_0^1 g'(su + (1-s)U)\, ds. \tag{3.2}$$

Notice that in N, an irregular function g is modified by smoothing. Let us consider now the following *linear dual problem*. Given u and U, find $z \in V$, so that

$$B(u, U; v, z) = (v(T), \|e(T)\|^{-1}e(T)) \quad \forall\, v \in V. \tag{3.3}$$

It is easily seen that the dual problem (3.3) corresponds to solving a quasi-hyperbolic problem backward in time, namely,

$$-z_t - M^T z_x = Dz_{xx} - \frac{1}{\tau} N^T z \quad \text{in} \quad \Omega \times I, \tag{3.4}$$

with initial and boundary conditions

$$z|_{t=T} = \|e(T)\|^{-1} e(T), \qquad z|_{x\in\{0,1\}} = 0. \tag{3.5}$$

This corresponds to a forward problem in reflected coordinates. The dual problem is now used to derive a representation for the error $e(T)$. To this end, we take $v = e$ in (3.3), obtaining

$$\|e(T)\| = B(u, U; e, z) = A_0(u; z) - A_0(U; z). \tag{3.6}$$

In the next step, we employ the Galerkin orthogonality of the SDFEM. The (smooth) exact solution u of (1.1) satisfies

$$A_0(u; v) = L(v), \qquad v \in V. \tag{3.7}$$

Consequently, there holds the perturbed orthogonality relation

$$B(u, U; e, v) = (A_\delta - A_0)(U, v), \qquad v \in V_h. \tag{3.8}$$

By means of this, (3.6) turns into

$$\|e(T)\| = L(z - Z) + (A_\delta - A_0)(U, z) - A_\delta(U, z - Z)$$

for any $Z \in V_h$. Writing this out, we obtain the error representation formula

$$\begin{aligned}\|e(T)\| = \sum_{n=1}^{N} \Bigg\{ &\left(U_t + f(U)_x + \frac{1}{\tau} g(U), Z - z + \delta\{Z_t + f'(U)^T Z_x\} \right)_n \\ &- \sum_{l=1}^{M_n} \int_{I_n} [DU_x]_{n,l} (Z - z)(t, x_{n,l})\, dt - ([U]_n, Z_n^+ - z_n) \Bigg\},\end{aligned} \tag{3.9}$$

where the $[DU_x]_{n,l}$ denote normal-jumps across grid lines $\{x_{n,l}\} \times I_n$, and $U_0^- := u_0$. The error representation (3.9) immediately leads us to an a posteriori error estimate. Applying elementwise the Cauchy–Schwarz inequality yields

$$\|e(T)\| \le \sum_{K\in Q} \left\{ \omega_K \left\| U_t + f(U)_x + \frac{1}{\tau} g(U) \right\|_K + \omega_\Gamma \|[DU_x]\|_\Gamma + \omega_L \|[U]\|_L \right\}, \tag{3.10}$$

with the local weights

$$\omega_K := \|Z - z + \delta\{Z_t + f'^T(U) Z_x\}\|_K, \qquad \omega_\Gamma := \|Z - z\|_\Gamma, \qquad \omega_L := \|Z^+ - z\|_L.$$

Here, the sum extends over all elements $K = K_{n,l} \in Q$, where Γ, $L \subset \partial K_{n,l}$ denote the line segments $\Gamma := \{x_{n,l}\} \times I_n$ and $L := I_{n,l} \times \{t_n\}$.

The error estimate (3.10) can be carried further by bounding the weights ω_K, ω_Γ, and ω_L using local interpolation estimates.

LEMMA 3.1. *Let $v \in H^1(I_{n,l})$ and $w \in H^1(K_{n,l})$ be scalar or vector functions and $I_h v$, $I_h w$ their linear and bilinear interpolants in the endpoints of $I_{n,l}$ and $K_{n,l}$, respectively. Then, there hold*

$$\|I_h v - v\|_{I_{n,l}} \le c_{I,1} h_{n,l} \|v_x\|_{I_{n,l}}, \tag{3.11}$$

$$\|I_h w - w\|_{K_{n,l}} \le c_{I,2} \left(k_n^2 \|w_t\|_{K_{n,l}}^2 + h_{n,l}^2 k_n \|w_x\|_{I_{n,l}\times\{t_{n,l-1}\}}^2 \right)^{1/2}, \tag{3.12}$$

with constants

$$\tfrac{1}{10}\sqrt{10} \le c_{I,1} \le \tfrac{1}{2}\sqrt{2}, \qquad \frac{1}{10}\sqrt{10} \le c_{I,2} \le 1.$$

Proof. For simplicity, we assume $I_{n,l} = (0,h)$ and $K_{n,l} = (0,h)\times(0,k)$. The lower bounds of $c_{I,1}$ and $c_{I,2}$ are obtained by using the model functions $v_0(x) = x(h-x)$ and $w_0(x,t) = x(h-x) + t(k-t)$, respectively. For proving the upper bounds, we assume without loss of generality that $v(0) = v(h) = 0$ and $w = 0$ in the corners of K. Then, by using $v(x) = \int_0^x v'(t)\,dt$ and $w(x,t) = \int_0^t w_s(x,s)\,ds + \int_0^x w_y(y,0)\,dy$ together with the Cauchy–Schwarz inequality, elementary calculations yield (3.11) and (3.12). ∎

Combining the foregoing estimates, we obtain the following main result.

THEOREM 3.2. *The SDFEM for problem* (1.1) *admits the a posteriori error estimate*

$$\|e(T)\| \le \sum_{K\in Q} \left\{ \left(c_{I,2}\omega_K^{(1)} + \delta_K \omega_K^{(2)} \right) \rho_K + c_{I,1}\omega_\Gamma \rho_\Gamma + c_{I,1}\omega_L \rho_L \right\} \tag{3.13}$$

with the local residual terms

$$\rho_K := \left\| U_t + f(U)_x + \frac{1}{\tau} g(U) \right\|_K, \qquad \rho_\Gamma := \|[DU_x]\|_\Gamma, \qquad \rho_L := \|[U]\|_L,$$

and weights

$$\omega_K^{(1)} := \left(k_K^2 \|z_t\|_K^2 + h_K^2 k_K \|z_x\|_L^2 \right)^{1/2}, \qquad \omega_K^{(2)} := \|(I_h z)_t + f'(U)^T (I_h z)_x\|_K,$$
$$\omega_\Gamma := k_\Gamma \|z_t\|_\Gamma, \qquad \omega_L := h_L \|z_x\|_L.$$

Here, the sum extends over all elements $K = K_{n,l} \in Q$, where Γ, $L \subset \partial K_{n,l}$ denote the line segments $\Gamma := \{x_{n,l-1}\} \times I_n$, and $L := I_{n,l} \times \{t_{n-1}\}$.

The a posteriori error bound (3.13) may be written in short as

$$\|e(T)\| \le \eta(U) := \sum_{K\in Q} \eta_K, \tag{3.14}$$

with the local *error indicators*

$$\eta_K := \left(c_{I,2}\omega_K^{(1)} + \delta_K \omega_K^{(2)} \right) \rho_K + c_{I,1}\omega_\Gamma \rho_\Gamma + c_{I,1}\omega_L \rho_L.$$

For evaluating the error bound (3.14), we need estimates for derivatives of the dual solution z. To this end, the dual problem is solved numerically by the same discretization procedure as used for the original problem. However, solving the dual problem requires us to store the discrete solution U on the whole space-time grid. Therefore, we replace the latter by a coarse grid approximation $\tilde{U}$ in both time and space. This

is expected to be feasible since the dual solution appears as weights in the error estimate only and may be less accurately approximated than the solution of the original problem. However, this may become critical when larger time steps are used. The coarse grid approximation further allows for extrapolating $U(T)$ appropriately to get a rough approximation to $e(T)$ for the dual problem.

Our numerical experiences of section 5 show the good quality of this estimate. Its correct sensitivity to the local mesh size $h_{n,l}$ as well as the streamline diffusion parameter δ is particularly valuable with regards to qualitatively correct mesh adaptivity. Practically, this estimate is evaluated on a coarser grid of doubled mesh size in both time and space, where z and $I_h z$ are replaced by the SDFEM approximate Z of the dual solution and its difference quotients, respectively. On large time intervals $[0,T]$, it can be too expensive to store U even on a coarser time grid. Then, one may apply the a posteriori error bound (3.14) successively on a sequence of macrotime intervals $[T_{r-1},T_r]$. However, in this case, the possible (linear) error accumulation as $r \to \infty$ is not controlled by the error estimation, but we expect essentially better results than without using macro time steps.

Although the error estimator (3.14) seems to correctly capture the qualitative behavior of the true error, it still leads to overestimation by factors between 2 and 5, which cannot be blamed only on an inappropriately large choice of the interpolation constants $c_{I,i}$ or on an inaccurate solution of the dual problem. Indeed, the quality of the error bound does not seem to depend much on the quality of the approximate dual solution but more on the accurate representation of the dual problem itself involving the computed solution U. We believe that at least two additional factors may be responsible for this critical overestimation:

1. In estimating the weights ω_K, ω_Γ, and ω_L, occurring in the first error bound (3.10), only first-order approximation in space and time is used which seems justified in view of the low degree of global regularity of the dual solution. However, the use of the full second order, $h_L^2\|z_{xx}\|$, $k_\Gamma^2\|z_{tt}\|$, at least in areas where z happens to be smooth, may further reduce the size of the error bound.

2. The weight $\omega_K^{(2)} = \|(I_h z)_t + f'(U)^T (I_h z)_x\|_K$ in (3.13) measuring the pollution effect of the local SD damping term may be unnecessarily large. The error analysis in [27] for general least-squares stabilized finite element schemes shows that the influence of such terms may be reduced by employing mesh-dependent duality arguments in the derivation of the a posteriori error estimates. However, this effect has not yet been fully understood.

These two options for sharpening our a posteriori error estimate have to be further investigated in future work.

The relative computational costs of solving the *linearized* dual problem depend strongly on the complexity of the original nonlinear primal problem. The additional costs are low in those cases where the nonlinearity of the primal problem requires many iteration sweeps per time step. Thus, the present approach to error estimation is particularly economical in the case of very complex applications. In the present model application of moderate complexity, assuming two nonlinear iterations per time step, the additional costs are moderate but not negligible. Due to the solution of the linear dual problem on a coarse grid only, they amount to about 20% of the total costs on the adapted mesh.

In the spatially multidimensional case storage considerations are required, since restoring all the history on U is then generally prohibitive. In this case, only regional averages of U on relatively large subdomains are manageable. The practical implica-

tions of this restriction is currently an open question.

We note that estimates for error functionals other than $\|e(\cdot,T)\|$ are easily derived by modifying the dual problem appropriately. For instance, to represent a component $\|e_i(\cdot,T)\|$, we just have to replace the final condition by

$$z|_{t=T} = \|v^{(i)}(T)\|^{-1} v^{(i)}(T),$$

where $v^{(i)}$ is the vector field with ith component e_i and all other components vanishing. Further, by using the final condition

$$z|_{t=T} = \delta_{x_0} w^{(i)},$$

where δ_{x_0} denotes the Dirac function at x_0 and $w^{(i)}$ the ith Euclidean unit vector, we get an error representation of $e_i(x_0,T)$. Examples of other error functionals are discussed in [2].

4. An adaptive algorithm. Our adaptive procedure is based on the error estimate of Theorem 3.2, i.e., it is optimized to approximate the solution at the final time, $u(\cdot,T)$. A crucial role in this procedure is played by the streamline diffusion parameter δ which is also successively adapted. Accordingly, we employ a two-stage concept of adaptivity:

1. *The finite element mesh is optimized by evaluating the error estimate.*
2. *The streamline diffusion parameter is used to optimize the overall quality.*

In the following schemes, TOL denotes a user-prescribed tolerance for the error $\|e(T)\|_\Omega$ to be controlled. Also, further parameters $\alpha \approx 1$ and $\beta > 0$ appear.

First, we describe step 1. The general idea is to improve a given mesh by generating a new mesh on which the local error indicators η_K in (3.14) are equidistributed.

Grid adaptation strategy.. The local error indicators η_K are computed for all elements $K \in Q$ resulting in an average value $\bar\eta$. If $\eta_K > \alpha\bar\eta$, the element K is split up into two equally sized subelements by bisecting the corresponding x-interval (but retaining the time step). Further, the element K is split in the same way if both spatial neighbors K' satisfy $\eta_{K'} > \alpha\bar\eta$ or if otherwise $|K| > 4|K'|$ would hold for at least one spatial neighbor. If $\eta_K < \frac{1}{5}\bar\eta$, K is eliminated from the mesh.

Numerical examples show that the outcome strongly depends on the particular choice of δ_K. Our further strategy is oriented by the observation that δ should be chosen *small* enough to ensure small consistency errors and to minimize the interaction between numerical diffusion and the sources, but on the other hand *large* enough to suppress the numerical oscillations of the standard Galerkin scheme. This raises the question of how to design a good strategy for computing δ adaptively. If no stiff source term were present, a *balancing strategy* would be appropriate by which the δ-dependent part of the error estimator is balanced with the remaining part. This has been investigated for the purely hyperbolic case in [11]. But this approach does not take into account the disastrous effect of the source terms which is unfortunately not explicitly reflected in the error estimator. Therefore, we follow a different simplified strategy. Let δ be varying from element to element like $\delta = c_{sd}h$, with a *streamline diffusion constant* c_{sd} and the variable mesh size h. Initially, we choose a small c_{sd}. At this stage we do not care about numerical oscillations which should disappear in the course of the algorithm. In further iterations c_{sd} is increased, so that both the actual error as well as its estimator decrease. The error should increase again when the numerical diffusion begins to interact with the source term. An iterative scheme based on such a strategy should lead to good approximation at moderate expense.

Our adaptive algorithm now combines the two strategies for adapting the mesh as well as the streamline diffusion parameter.

Adaptive algorithm.

1. *Start with an initial quadrangulation* $Q^{(1)}$. *Set* $s := 1$.
2. *Start with a small* $c_{sd}^{(s,1)}$. *Set* $\nu := 1$.
3. *Compute the discrete solution* $U^{(s,\nu)}$ *by the SDFEM.*
4. *Compute the dual solution* Z *and evaluate the error estimator* $\eta(U^{(s,\nu)})$.
5. *If* $\eta(U^{(s,\nu)}) < \eta(U^{(s,\nu-1)})$, *then*
   If $\eta(U^{(s,\nu)}) > TOL$, *set* $c_{sd}^{(s,\nu+1)} := (1+\beta)c_{sd}^{(s,\nu)}$, *and* $\nu := \nu + 1$. *Go to* 3.
   Else, accept $U^{(s,\nu)}$. *Stop.*
6. *If* $\eta(U^{(s,\nu)}) \geq \eta(U^{(s,\nu-1)})$, *then*
   Generate new $Q^{(s+1)}$ *from the values* $\eta_K^{(s,\nu-1)}$ *according to the grid adaption strategy.*
   Set $c_{sd}^{(s+1,1)} := c_{sd}^{(s,\nu-1)}$, $s := s+1$, *and* $\nu := 1$. *Go to* 3.

We will report on numerical experience with this algorithm in the following section.

5. Numerical experiments. As a prototypical application, we consider a relatively simple one-dimensional model for the propagation of detonation waves, where

$$u = (\rho, m, e, \sigma)^T$$

consists of the conservative Euler variables: density ρ, momentum m ($m = \rho v$, with velocity v), total energy density e, and fuel density σ. Detonation waves are governed by the differential system (omitting diffusive forces) [13],

$$\rho_t + m_x = 0, \tag{5.1}$$

$$m_t + \left(\frac{m^2}{\rho} + p\right)_x = 0, \tag{5.2}$$

$$e_t + \left(\frac{m}{\rho}(e+p)\right)_x = 0, \tag{5.3}$$

$$\sigma_t + \left(\frac{m}{\rho}\sigma\right)_x = -\frac{1}{\tau}H_I(\Theta)\sigma, \tag{5.4}$$

where $\sigma = \rho Z$, with the fuel concentration $0 \leq Z \leq 1$, with the extreme cases $Z = 0$ and $Z = 1$ meaning burnt or unburnt gas, respectively. The pressure p and the temperature Θ are obtained from the relations

$$\Theta = \frac{p}{\rho\mathcal{R}}, \qquad e = \frac{p}{\gamma - 1} + 0.5\frac{m^2}{\rho} + q_0\sigma. \tag{5.5}$$

In the source term, we used a Heaviside jump-function, $H_I(\Theta)=1$ where $\Theta > \Theta_I$ and $H_I(\Theta) = 0$ elsewhere, as an idealized variant of Arrhenius's ignition model (Θ_I the ignition temperature).

The profile of the detonation wave, the *ZND structure*, is obtained by omitting the time derivatives from the differential system and integrating it explicitly in the moving reference frame. This leads to a nonlinear ODE for the σ-variable (cf. [13]) to get the initial data.

All numerical experiments are carried out with (5.1)–(5.4) at still moderate relaxation times $\tau = 10^{-1}$ and $\tau = 10^{-2}$. We set $\mathcal{R} = q_0 = 1, \gamma = 1.4$, and the ignition

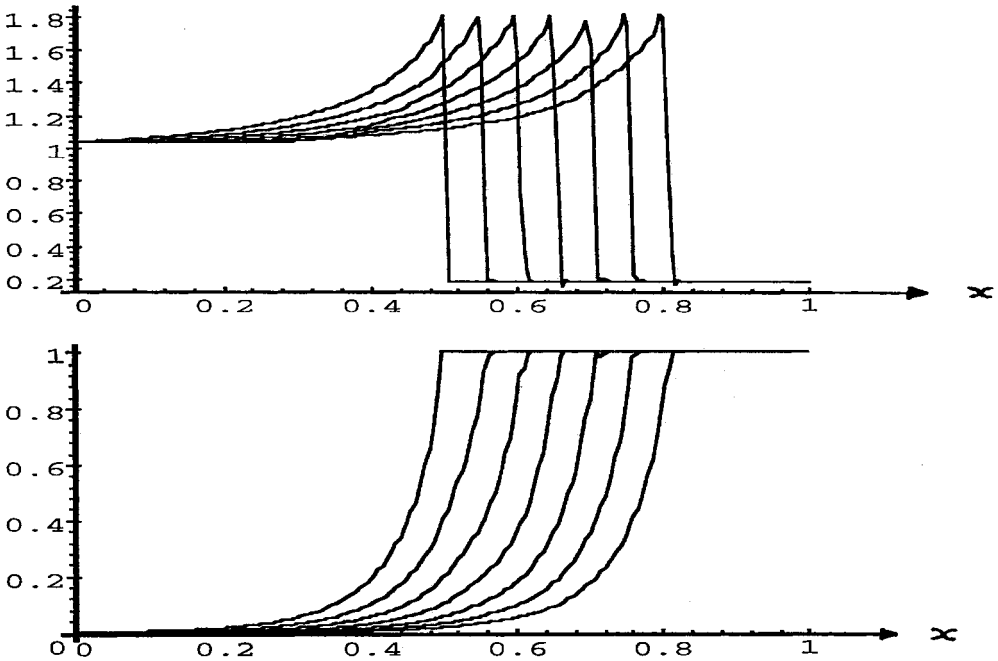

FIG. 2. *Travelling pressure wave and fuel concentration shown after* $N = 0, 10, \ldots, 60$ *time steps for the case* $\tau = 10^{-1}$.

temperature $\Theta_I = 0.22$. The detonation wave is travelling with Chapman–Jouguet speed $v_{CJ} = 1$. The boundary data are in the laboratory frame as follows [22]:

$$\begin{aligned} \rho_{left} &= 1.4, & \rho_{right} &= 0.887564, \\ v_{left} &= 0.0, & v_{right} &= -0.577350, \\ p_{left} &= 1.0, & p_{right} &= 0.191709. \end{aligned}$$

Since $\Theta_I \approx \Theta_{right} = 0.216$, these data represent the *hard test case* with numerical diffusion strongly interacting with the source term.

First, we present some results with SDFEM applied to detonation waves, obtained on a uniform and relatively fine grid with mesh size

$$h = k = 0.005.$$

The initial data are obtained by solving the nonlinear ODE. A streamline diffusion parameter $\delta = 0.3 \cdot h$ has been used (on the basis of numerical experience). Figure 2 shows the pressure wave of the detonation and the corresponding fuel concentration wave. These results show that SDFEM is able to treat the propagation of detonation waves.

Next, we turn to some numerical experiments with our a posteriori error estimator. Since the detonation wave is known analytically (assuming that the nonlinear ODE for the initial data is solved exactly), we may compare our error estimator, named *EST*, with the actual error, $ERR = \|e(T)\|$. Notice that the L^2-error is necessarily large, of order $O(h^{0.5})$, because the solution is discontinuous (cf. Table 1).We have tested the sensitivity of our error estimator as a function of one varying parameter. The results are shown in Figure 3. These computations have been done, at first, for fixed $T = 0.1$, corresponding to $N = 20$ time steps of size $k = 0.005$ and using a

TABLE 1

Convergence history of the adaptive algorithm in the case $\tau = 10^{-1}$ (s, ν numbers of outer or inner cycle, respectively).

s	ν	c_{sd}	ERR	EST
1	1	0.020	0.527	1.748
	2	0.027	0.489	1.508
	3	0.035	0.456	**1.495**
	4	0.047	0.417	1.522
2	1	0.035	0.332	1.657
	2	0.047	0.279	1.338
	3	0.063	0.232	1.144
	4	0.083	0.235	**1.122**
	5	0.111	0.288	1.192
3	1	0.083	0.310	1.729
	2	0.111	0.286	1.587
	3	0.138	0.283	1.561
	4	0.173	0.241	1.488
	5	0.216	0.179	1.455
	6	0.249	0.145	1.428
	7	0.286	0.110	**1.378**
	8	0.329	0.167	1.482
4	1	0.286	0.367	0.605
	2	0.329	0.363	0.554
	3	0.378	0.288	0.467
	4	0.435	0.200	0.382
	5	0.500	0.192	0.356
	6	0.550	0.122	**0.277**
	7	0.605	0.114	0.298

fixed uniform partition into $M = 120$ spatial intervals. The first result is obtained at (nearly) vanishing diffusion, in order to observe the influence of c_{sd}. The subsequent figures show the results for varying $M = h^{-1} = 60 - 240$ and $T = 0.05 - 0.3$. We observe good agreement of both ERR and EST in most cases. Only little diffusion (ϵ_i of order 10^{-3}) is used in order to be more independent of c_{sd}.

All these results show that our error estimator (3.13) overestimates the true error by factors of 2–5 only (at least on short time intervals). Even more important for adaptivity is the error estimator's strong sensitivity for varying parameters.

At first, we report on tests with the adaptive algorithm for the moderately stiff case $\tau = 10^{-1}$. The time step is taken constant, $k = 0.0025$, in accordance with the accuracy requirements. All computations are carried out for vanishing diffusion. We choose the parameter values $\alpha = 0.9$ and β varying between 0.33 and 0.15 as a monotonically decreasing function of c_{sd}. We start ($s = 1$) with a nearly uniform mesh (see Figure 4) which, in view of the irregular initial data, is slightly graded near the detonation front. At the beginning, the streamline diffusion parameter is chosen as small as $c_{sd} = 0.02$. We do not care about the resulting numerical oscillations appearing on the coarsest grid.

We carry out four outer iteration sweeps resulting in three stages of grid refinement ($s = 2, 3, 4$). The complete history of the adaptive process is shown in Table 1. Our adaptive scheme reduces the L^2-error by a factor of 0.2, while merely doubling the number of unknowns. We note that on all grids the optimal values of c_{sd} nearly coincide for both the error estimator and the actual error. This important phenomenon, seen from Table 1, to some extent justifies our approach of simultaneously adapting the mesh size and the damping parameter. It would be interesting to investigate the possibility of adapting c_{sd} also locally on the mesh. It is worth noting that the op-

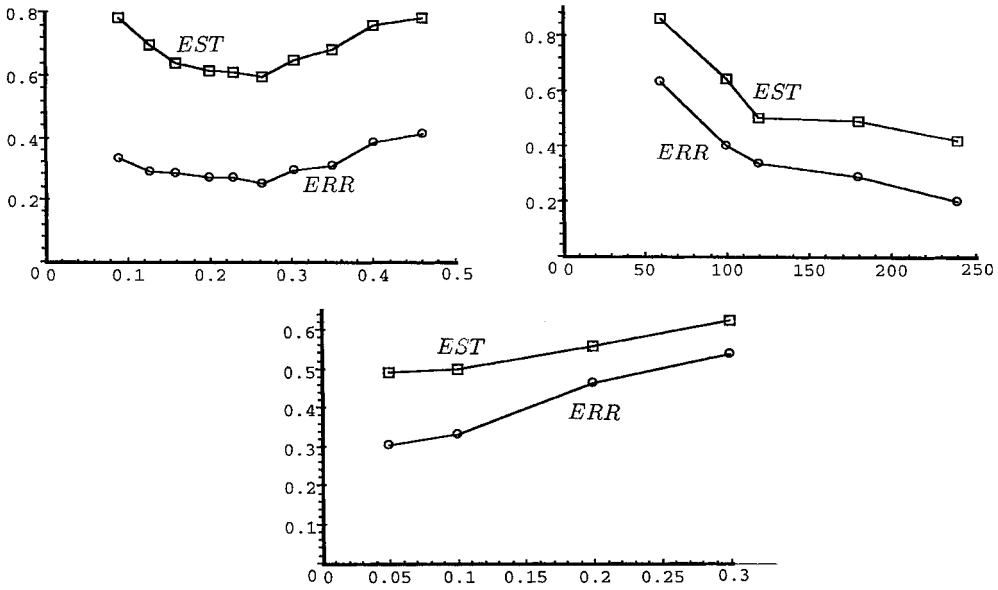

FIG. 3. *Estimated vs. actual error* $ERR = \|e\|$, *as functions of* c_{sd} *(upper left),* $M = h^{-1}$ *(upper right), and* T *(lower middle).*

timal value of c_{sd} seems to increase with proceeding grid refinement and increasing accuracy of the discretization. This effect should be exploited for reducing the number of iterations in practical cases.

Some details of this procedure are shown in Figures 4–7. We begin with the obtained approximation of the pressure profile on each grid, for the first 40 time steps, compared to the exact initial data. On the initial grid ($s = 1$), a poor approximation of the pressure wave is produced; see Figure 4. Nevertheless, it is still good enough to serve as basis for error estimation and grid refinement. The resulting new grid is seen in Figure 5. The best result for the pressure wave is obtained at $s = 4$, as seen in Figure 7. It compares well with the result obtained on the uniform fine grid (Figure 2) but requires only 30% of the grid points. The corresponding mesh, Figure 7, clearly shows good refinement near the position $x = 0.5 + t$ of the detonation front.

Finally, we repeat the whole computation for the harder case $\tau = 10^{-2}$. The results are shown in Figures 8–10. In order to speed up the refinement process, the initial mesh has been even more graded toward the front position. In accordance to the very small minimum mesh size the (constant) time step is now chosen as $k = h_{min} = 0.00025$. Error control is accomplished using 10 macrotime intervals $[T_{r-1}, T_r]$ each of which consists of 40 microtime DG(1) steps. In each of these macrotime intervals the computation is started from a graded spatial mesh of type as shown in Figure 8 with the current approximation $U(t_{r-1})$ as initial value.

The resulting refined meshes and corresponding pressure profiles obtained with optimized diffusion c_{sd} are shown in Figures 8–10. For brevity, we show the meshes (actually a zoom of the mesh in the neighborhood of the front) only for the first macrotime interval. The others look similar. Our adaptive mesh-refinement strategy leads to a good resolution of the detonation front with relatively little increase in numbers of mesh points. Finally, the convergence history of the adaptive algorithm is displayed in Table 2. Again, it turns out that the a posteriori error bound (3.14) is

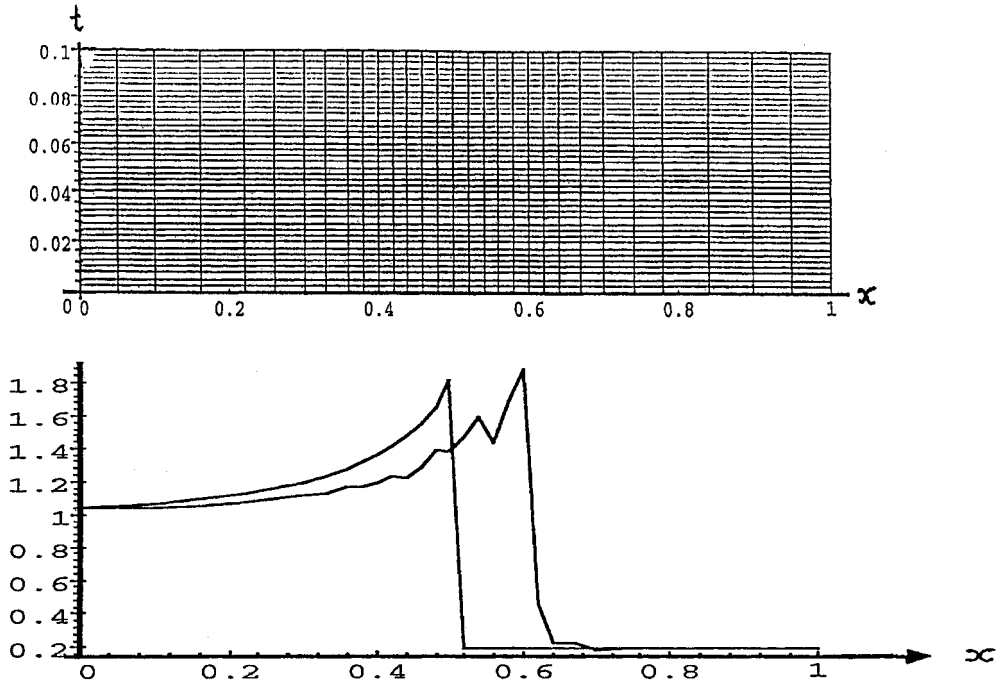

FIG. 4. *Initial quadrangulation* $Q^{(1)}$ *and corresponding pressure distribution* $p^{(1)}$ *at time* $t_0 = 0$ *and after* 40 *time steps at time* $T = 0.1$, *for* $\tau = 10^{-1}$.

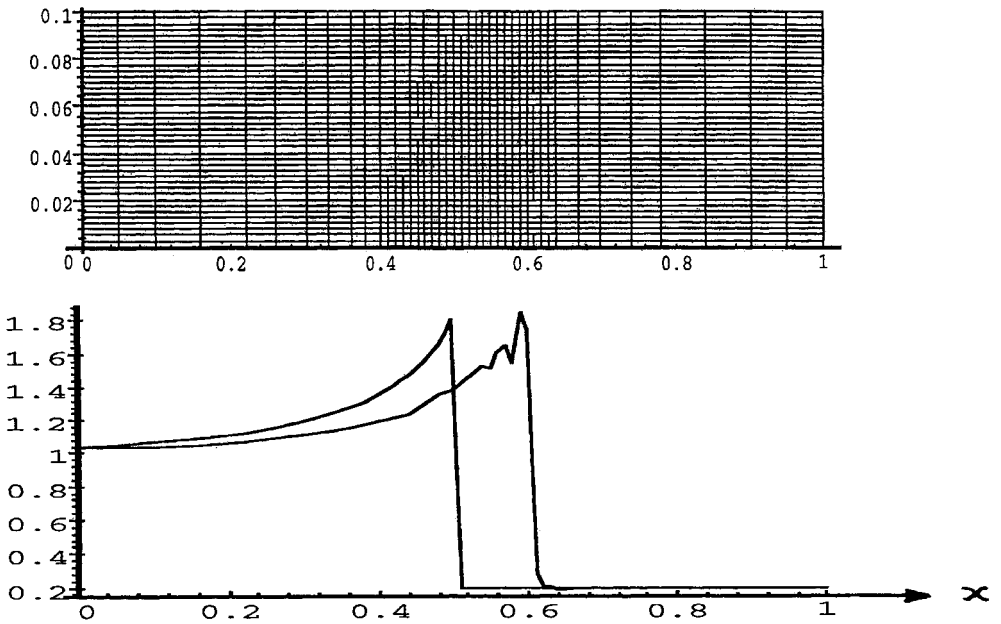

FIG. 5. *Refined quadrangulation* $Q^{(2)}$ *and corresponding pressure distribution* $p^{(2)}$ *at time* $t_0 = 0$ *and after* 40 *time steps at time* $T = 0.1$, *for* $\tau = 10^{-1}$.

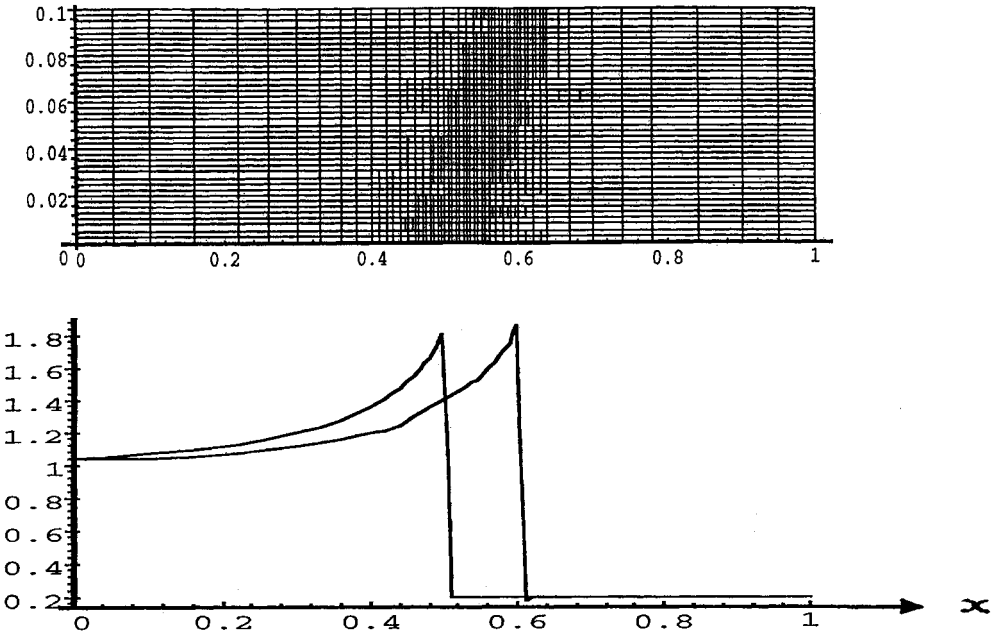

FIG. 6. *Refined quadrangulation* $Q^{(3)}$ *and corresponding pressure distribution* $p^{(3)}$ *at time* $t_0 = 0$ *and after* 40 *time steps at time* $T = 0.1$, *for* $\tau = 10^{-1}$.

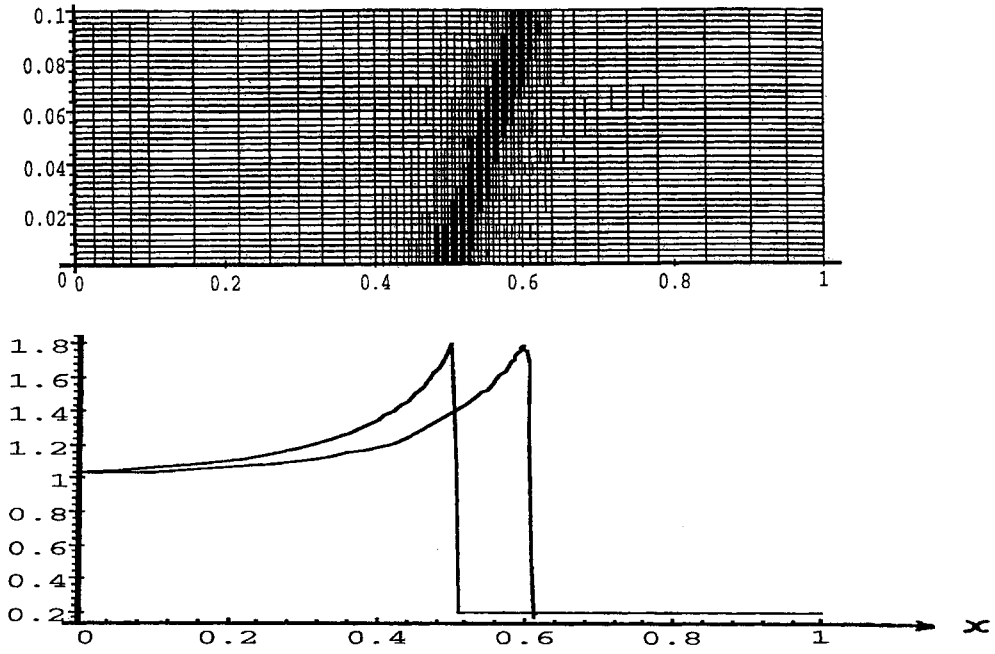

FIG. 7. *Refined quadrangulation* $Q^{(4)}$ *and corresponding pressure distribution* $p^{(4)}$ *at time* $t_0 = 0$ *and after* 40 *time steps at time* $T = 0.1$, *for* $\tau = 10^{-1}$.

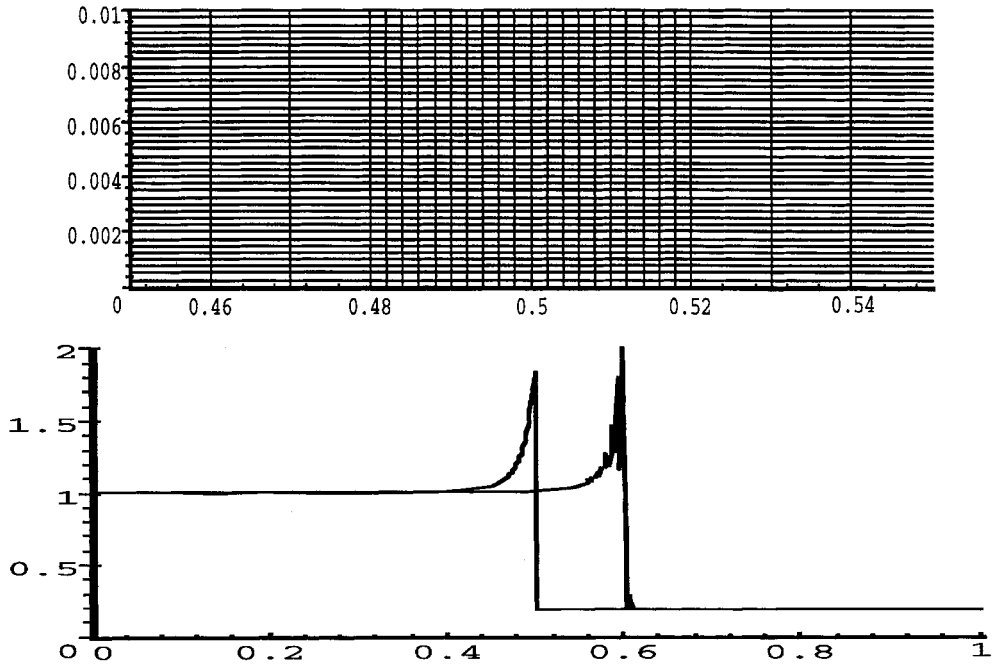

FIG. 8. *Initial quadrangulation* $Q^{(1)}$ *and corresponding pressure distribution* $p^{(1)}$ *at the time* $t_0 = 0$ *and after* 10×40 *time steps at* $T = 0.1$, *for* $\tau = 10^{-2}$.

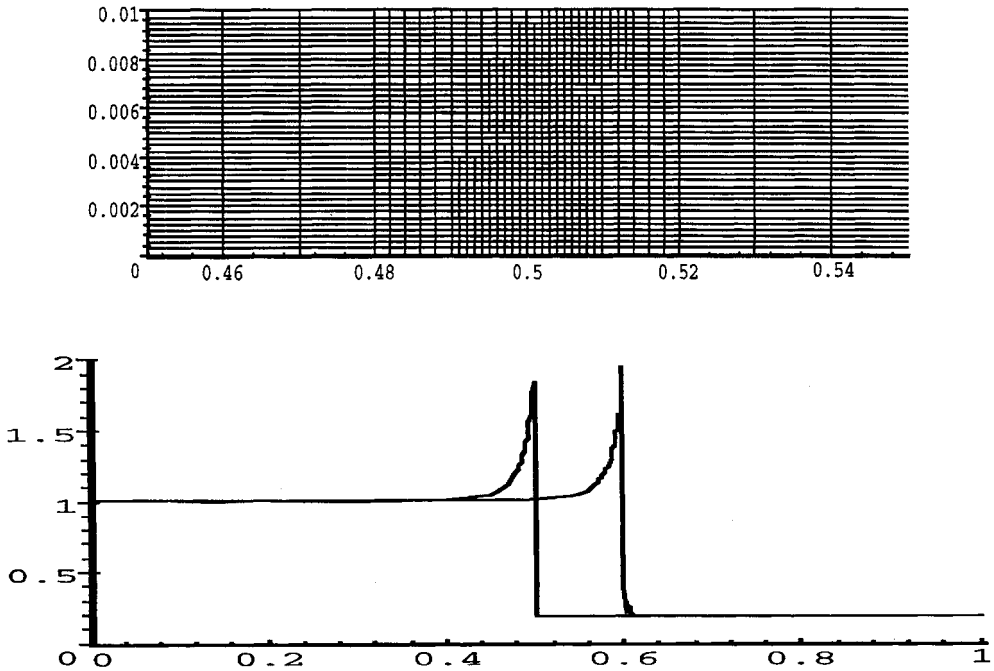

FIG. 9. *Refined quadrangulation* $Q^{(2)}$ *and corresponding pressure distribution* $p^{(2)}$ *at the time* $t_0 = 0$ *and after* 10×40 *time steps at* $T = 0.1$, *for* $\tau = 10^{-2}$.

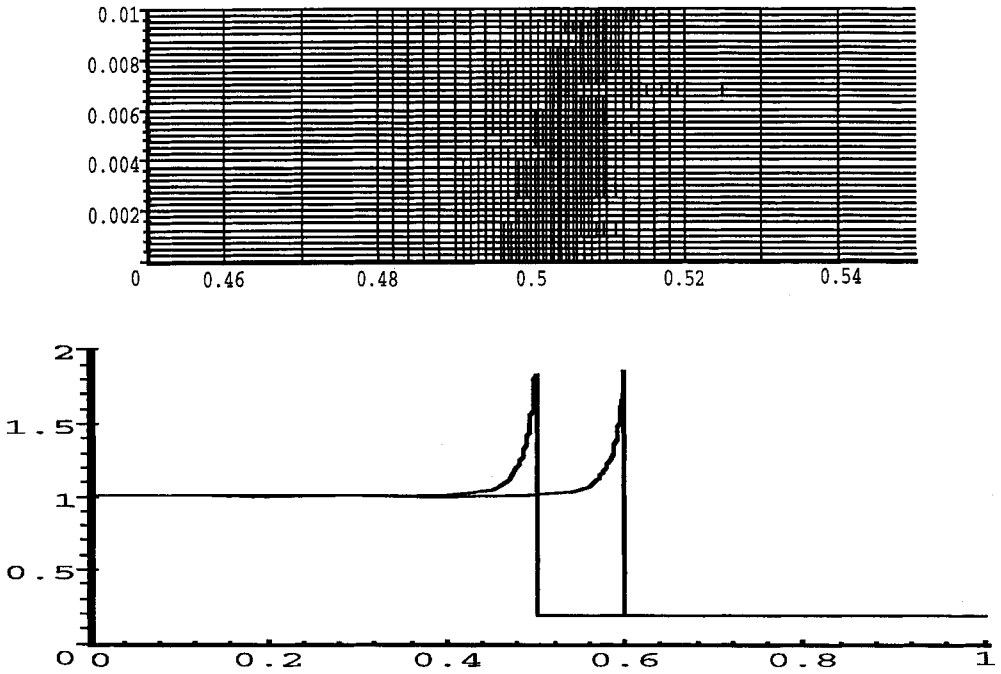

FIG. 10. *Refined quadrangulation* $Q^{(3)}$ *and corresponding pressure distribution* $p^{(3)}$ *at the time* $t_0 = 0$ *and after* 10×40 *time steps at* $T = 0.1$, *for* $\tau = 10^{-2}$.

TABLE 2

Convergence history of the adaptive algorithm in the case $\tau = 0.01$ *(*s, ν *numbers of outer or inner cycle, respectively).*

s	ν	c_{sd}	ERR	EST
1	1	0.020	0.170	0.548
	2	0.027	0.157	**0.474**
	3	0.035	0.147	0.477
2	1	0.027	0.128	0.726
	2	0.035	0.108	0.604
	3	0.047	0.088	0.495
	4	0.063	0.079	0.431
	5	0.083	0.073	**0.390**
	6	0.111	0.078	0.393
3	1	0.083	0.157	0.411
	2	0.111	0.141	0.365
	3	0.138	0.135	0.316
	4	0.173	0.122	0.249
	5	0.216	0.103	0.227
	6	0.249	0.090	0.208
	7	0.286	0.075	**0.171**
	8	0.329	0.087	0.195

remarkably accurate with an overestimation factor ranging between 2 and 5.

The case of very small τ ($\approx 10^{-6}$) has been addressed in the recent paper [14]. Yet, in the *nonchaotic case* $\Theta_I \gg \Theta_{right}$, it turns out that these problems are manageable as well, but require additional mesh-coarsening and weakening of the relation $\delta \approx h$. In fact, a *balancing strategy* has been employed to fix δ. It should be noticed that extremely nonuniform meshes appear, thus invoking the question of how to get

reasonable initial meshes. In any case, all these partly open problems underline the necessity of developing adaptive strategies based on accurate error estimation.

Acknowledgment. We wish to thank an anonymous referee for careful comments which helped to clarify the presentation of our results.

REFERENCES

[1] J. Bebernes and D. Eberly, *Mathematical Problems from Combustion Theory*, Springer, New York, 1989.

[2] R. Becker and R. Rannacher, *Weighted a posteriori error control in FE methods*, in Proceedings ENUMATH-97, Heidelberg, 1997, World Scientific, Singapore, 1998.

[3] R. Becker and R. Rannacher, *A feed-back approach to error control in finite element methods: Basic analysis and examples*, East-West J. Numer. Math., 4 (1996), pp. 237–264.

[4] K. Böttcher and R. Rannacher, *Adaptive Error Control in Solving Ordinary Differential Equations by the Discontinuous Galerkin Method*, Preprint 96–53, SFB 359, Universität Heidelberg, Heidelberg, Germany, 1996.

[5] A. J. Bourlioux, A. J. Majda, and V. Roytburd, *Theoretical and numerical structure for unstable one-dimensional detonations*, SIAM J. Appl. Math., 51 (1991), pp. 303–343.

[6] P. Colella, A. Majda, and V. Roytburd, *Theoretical and numerical structure for reacting shock waves*, SIAM J. Sci. Statist. Comp., 7 (1986), pp. 1059–1080.

[7] R. Courant and K. O. Friedrichs, *Supersonic Flow and Shock Waves*, Interscience, New York, 1948.

[8] K. Eriksson and C. Johnson, *Adaptive finite element methods for parabolic problems.* I. *A linear model problem*, SIAM J. Numer. Anal., 28 (1991), pp. 43–77.

[9] K. Eriksson and C. Johnson, *Adaptive finite element methods for parabolic problems.* IV. *Nonlinear Problems*, SIAM J. Numer. Anal., 32 (1995), pp. 1729–1749.

[10] K. Eriksson, D. Estep, P. Hansbo, and C. Johnson, *Introduction to adaptive methods for differential equations*, Acta Numerica, 1995, pp. 105–159.

[11] C. Führer and R. Rannacher, *An adaptive streamline–diffusion finite element method for hyperbolic conservation laws*, East-West J. Numer. Math., 5 (1997), pp. 145–162.

[12] R. Gathmann and F. K. Hebeker, *Numerical problems of a convection diffusion equation with Arrhenius source term*, in Proceeding of the Fifth European Conference on Mathematics in Industry, M. Heiliö, ed., Teubner, Stuttgart, 1991, pp. 229–233.

[13] E. Godlewski and P. A. Raviart, *Numerical Approximation of Hyperbolic Systems of Conservation Laws*, Springer, Berlin, Heidelberg, New York, 1996.

[14] F. K. Hebeker, *An Adaptive Finite Element Method for Detonation Waves: Towards Reaction Time Limit Zero*, Preprint 98–27, SFB 359, Universität Heidelberg, Heidelberg, Germany, 1998.

[15] F. K. Hebeker, R. Maly, and S. Schöffel, *Numerical simulation of knock damage phenomena on an IBM RS/*6000 *workstation cluster*, in Proceedings 26th International Symposium on Automotive Technology and Automation, Automotive Automation, Croydon, 1993, pp. 275–282.

[16] J. Hildtich and P. Colella, *A front tracking method for compressible flames in one dimension*, SIAM J. Sci. Comput., 16 (1995), pp. 755–772.

[17] C. Hirsch, *Numerical Computations of Internal and External Flows*, Wiley, Chichester, 1990.

[18] T. J. R. Hughes, L. P. Franca, and M. Mallet, *A new finite element formulation for computational fluid dynamics:* I. *Symmetric forms of the compressible Euler and Navier–Stokes equations and the second law of thermodynamics*, Comput. Methods Appl. Mech. Engrg., 54 (1986), pp. 223–234 .

[19] C. Johnson, *Numerical Solution of Partial Differential Equations by the Finite Element Method*, Cambridge University Press, Cambridge, UK, 1987.

[20] C. Johnson and A. Szepessy, *Adaptive finite element methods for conservation laws based on a posteriori error estimates*, Comm. Pure Appl. Math., 48 (1995), pp. 199–234.

[21] G. Kanschat, *Solution of multi-dimensional radiative transfer problems on parallel computers*, in Parallel Solution of Partial Differential Equations, IMA Vol. Math. Appl., Springer-Verlag, New York, to appear.

[22] R. LeVeque, *Numerical Methods for Conservations Laws*, 2nd ed., Birkhäuser Verlag, Basel, 1990.

[23] R. J. LeVeque and K. M. Shuye, *One-dimensional front tracking based on high resolution wave propagation methods*, SIAM J. Sci. Comput., 16 (1995), pp. 348–377.

[24] R. LeVeque and H. Yee, *A study of numerical methods for hyperbolic conservation laws with stiff source terms*, J. Comput. Phys., 86 (1990), pp. 187–210.
[25] J. D. Murray, *On the Gunn effect and other physical examples of perturbed conservation laws*, J. Fluid Mech., 44 (1970), pp. 315–346.
[26] R. B. Pember, *Numerical methods for hyperbolic conservation laws with stiff relaxation.* II. *Higher-order Godunov methods*, SIAM J. Sci. Comput., 14 (1993), pp. 824–859.
[27] R. Rannacher, *A posteriori error estimation in least-squares stabilized finite element schemes*, Comput. Methods Appl. Mech. Engrg., 166 (1998), pp. 99–114.
[28] R. Rannacher and F.-T. Suttmeier, *A feed-back approach to error control in finite element methods: Application to linear elasticity*, Comput. Mech., 19 (1997), pp. 434–446 .
[29] R. Rannacher and G. Zhou, *Pointwise superconvergence of the streamline diffusion finite-element method*, Numer. Methods Partial Differential Equations, 12 (1996), pp. 123–145.
[30] R. Sandboge, *Adaptive Finite Element Methods for Reactive Flow Problems*, Ph.D. thesis, Chalmers University of Technology, Gothenburg, 1996.
[31] K. Strehmel and R. Weiner, *Numerik gewöhnlicher Differentialgleichungen*, Teubner, Stuttgart, 1995.
[32] W. A. Yong, *Singular Perturbations of First-Order Hyperbolic Systems*, Ph.D. thesis, SFB 359, Universität Heidelberg, Heidelberg, Germany, 1992.
[33] G. Zhou, *How accurate is the streamline diffusion finite element method?*, Math. Comp., 66 (1996), pp. 31–44.